3

Spin-spin coupling

3.1 Introduction

Chapter 2 may have given the impression that the appearance of liquid-state NMR spectra is determined solely by chemical shifts—one resonance for each distinct nuclear environment. In fact, there is another extremely valuable source of information encoded in most NMR spectra, namely the magnetic interactions between nuclei, known variously as *spin-spin couplings*, *scalar couplings*, or *J-couplings*. Amongst other things, these interactions cause the ¹H spectrum of liquid ethanol to comprise not three (Fig. 1.1) but eight (and sometimes more) resonances when recorded at high resolution (Fig. 3.1).

3.2 Effect on NMR spectra

As Fig. 3.1 suggests, nuclear spin-spin coupling causes NMR lines to split into a small number of components with characteristic relative intensities and spacings. In the case of ethanol, the CH₃ peak becomes a *triplet*—three equally spaced

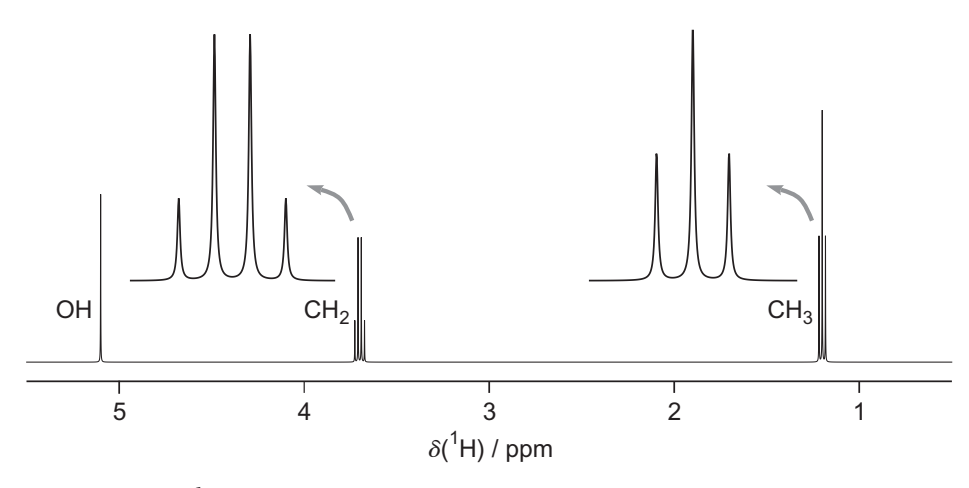


Fig. 3.1 400 MHz ¹H NMR spectrum of liquid ethanol showing the fine structure produced by spin–spin coupling. Compare this spectrum with Fig. 1.1, in which the splittings are obscured by instrumental linebroadening. Further structure appears in the spectrum when all traces of acid or base are removed (Fig. 4.12).

lines with relative amplitudes in the ratio 1:2:1—and the CH_2 resonance is split into a *quartet*—four equally spaced lines with relative intensities 1:3:3:1. To see how this *multiplet* structure arises we focus initially on a much simpler molecule, the formate ion HCO_2 in which the carbon is ^{13}C .

On the basis of the previous chapter, we might expect to see a single NMR line in each of the ¹H and ¹³C spectra. In fact both spins give rise to 'doublets': two lines disposed symmetrically either side of the chemical shift position, as shown in Fig. 3.2. The splitting (195 Hz in this case) is the strength of the ¹H-¹³C spinspin interaction and is the same for both spectra.

The ¹H resonance is split into two because the magnetic moment of the ¹³C produces a small local magnetic field at the position of the ¹H. When the ¹³C is in its $m = +\frac{1}{2}$ state (here denoted $C \uparrow$), it generates a magnetic field that opposes the external field and shifts the ¹H resonance to the right in Fig. 3.3. Conversely, for an $m = -\frac{1}{2}$ carbon ($C \downarrow$), the local field adds to the external field and moves the ¹H resonance in the opposite direction. In the language of chemical shifts, a $C \uparrow$ carbon shields the ¹H and a $C \downarrow$ carbon deshields it. The two components of the ¹H doublet thus correspond to two sorts of H¹³CO₂ molecule: those with $C \uparrow$ and those with $C \downarrow$. Since the difference in energy between the two configurations of the ¹³C spin is tiny compared to $k_B T$, the two kinds of H¹³CO₂ are equally likely, and the two components of the ¹H doublet are equally intense. An exactly analogous argument explains the splitting of the ¹³C resonance by the ¹H.

It is evident from Fig. 3.3 that the spin–spin interaction in $H^{13}CO_2^-$ stabilizes the antiparallel arrangements of nuclear spins ($H^{\uparrow}C^{\downarrow}$ and $H^{\downarrow}C^{\uparrow}$) and destabilizes the parallel configurations ($H^{\uparrow}C^{\uparrow}$ and $H^{\downarrow}C^{\downarrow}$). Thus the two energy levels of the proton ($m = \pm \frac{1}{2}$) are each split into two, with energies determined by the relative orientations of the ^{13}C and ^{1}H spins. The ^{1}H NMR transitions ($H^{\uparrow}C^{\uparrow} \rightarrow H^{\downarrow}C^{\uparrow}$) of molecules containing a C^{\uparrow} have a lower energy because the transition is from an energetically unfavourable state (parallel spins) to a favourable one (antiparallel spins). Conversely, molecules containing C^{\downarrow} have higher energy ^{1}H transitions ($H^{\uparrow}C^{\downarrow} \rightarrow H^{\downarrow}C^{\downarrow}$).

A *heteronuclear* example (¹H-¹³C) has been used to illustrate the nature of *J*-coupling merely as a matter of convenience; *homonuclear* couplings, e.g. between two protons with different chemical shifts, give rise to splittings in exactly the same way.

The properties of spin-spin coupling as illustrated by $H^{13}CO_2^-$ may be summarized and generalized in the following simple expression for the energy levels of two interacting nuclei A and X (not necessarily spin- $\frac{1}{2}$):

$$E(m_{A}, m_{X}) = m_{A}hv_{0A} + m_{X}hv_{0X} + hJ_{AX}m_{A}m_{X}$$
(3.1)

in which m_A and m_X are the magnetic quantum numbers of the two nuclei and v_{0A} and v_{0X} are the Larmor frequencies (eqn 2.4). J_{AX} is the strength of the interaction, known as the *spin-spin coupling constant* or the *J-coupling constant*. It is measured in frequency units (Hertz) and may be positive or negative: if the antiparallel arrangement of nuclear spins is energetically favoured, then $J_{AX} > 0$ (as in $H^{13}CO_2^-$); when the parallel spin configuration is lower in energy, $J_{AX} < 0$.

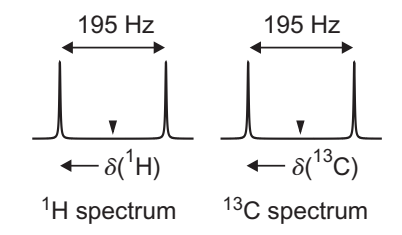


Fig. 3.2 ¹H and ¹³C spectra of H ¹³CO₂⁻ showing the doublets produced by ¹H-¹³C *J*-coupling. The arrowheads indicate the chemical shift positions at the centre of each doublet.

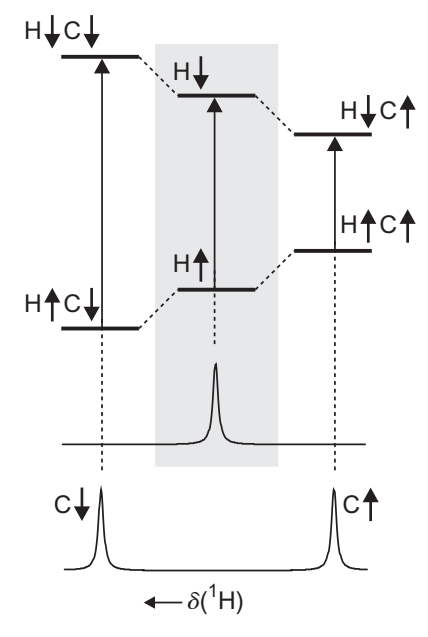


Fig. 3.3 The effect of ¹H-¹³C J-coupling in H¹³CO₂ on the energy levels and spectrum of the ¹H spin. For clarity, the energy-level shifts due to the J-coupling have been greatly exaggerated. The central pair of energy levels and the upper spectrum are appropriate in the absence of a spin-spin interaction. J-coupling produces the energy levels on the left and right, and the lower spectrum.

Eqn 3.1 is valid when $|v_{0A} - v_{0X}| \gg |J_{AX}|$. See Section 3.5.

Combining eqn 3.1 with the selection rule $\Delta m_{\rm A} = \pm 1$, one can see that the A–X interaction shifts the Larmor frequency of spin A ($v_{0,\rm A}$, eqn 2.4) by $J_{\rm AX}m_{\rm X}$. More generally, the equation for the resonance frequency becomes:

$$v_{A} = v_{0A} + \sum_{K \neq A} J_{AK} m_{K} \tag{3.2}$$

where the summation runs over all spins (K) that have an non-negligible *J*-coupling with A.

Fig. 3.4 shows the complete energy-level diagram and the corresponding NMR spectra for a pair of spin- $\frac{1}{2}$ nuclei with and without *J*-coupling. Note that the allowed transitions are those in which just one spin changes its magnetic quantum number ($\Delta m_A = \pm 1$ or $\Delta m_X = \pm 1$). Simultaneous changes in m_A and m_X , i.e. $A \uparrow X \uparrow \leftrightarrow A \downarrow X \downarrow$ and $A \uparrow X \downarrow \leftrightarrow A \downarrow X \uparrow$, are forbidden.

It should be clear from eqns 3.1 and 3.2 that the *sign* of the coupling constant has no effect on the appearance of the spectrum. For example, changing J_{AX} in

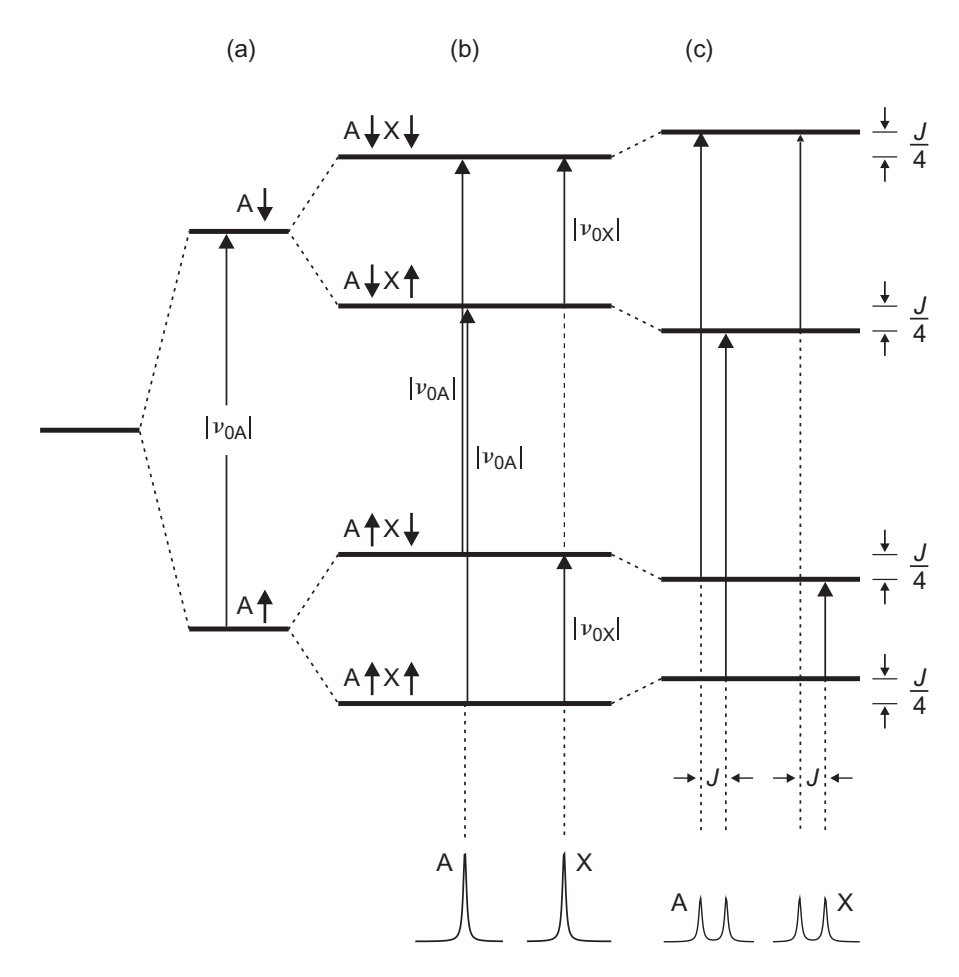


Fig. 3.4 Energy levels and spectra of a pair of spin- $\frac{1}{2}$ nuclei, A and X. From left to right, magnetic interactions are introduced in the order: (a) the interaction of A with the magnetic field B_0 ; (b) the interaction of X with B_0 ; (c) the spin-spin coupling, $J = J_{AX}$. For clarity, the energy-level shifts are not drawn to scale. v_{0A} and v_{0X} are the Larmor frequencies of the two spins in the absence of coupling. The shifts in the energy levels are given as frequencies. The figure is drawn for $\gamma_A > 0$, $\gamma_X > 0$ (so that v_{0A} and v_{0X} are both negative) and $J_{AX} > 0$.

Remember that $v_{0A} < 0$ for a nucleus with $\gamma_A > 0$, so that when $J_{AK}m_K > 0$, the resonance is shifted in the direction of increasing, i.e. less negative, frequency and thus moves to the right in the spectrum.

27

Fig. 3.4 from positive to negative simply interchanges the two components of each doublet.

These simple ideas, exemplified by H¹³CO₂, and embodied in eqns 3.1 and 3.2, allow one to predict the effect of spin-spin coupling on the NMR spectrum of almost any molecule. The exceptions will be dealt with later (Section 3.5).

3.3 Multiplet patterns

Having seen that coupling between nuclear spins can affect NMR spectra, we now look at some frequently encountered spin systems (collections of coupled nuclei) to see how they give rise to distinctive multiplets (doublets, triplets, quartets, etc.).

At this stage it is assumed that all pairs of spins are *weakly coupled*, i.e. that the difference in Larmor frequencies of the two nuclei, $|v_{0A} - v_{0X}|$, greatly exceeds their mutual coupling, $|J_{AX}|$. The complications associated with *strong coupling* are discussed in Section 3.5. All nuclei are spin- $\frac{1}{2}$, unless otherwise stated. The term *equivalent nuclei* is used to describe spins in identical environments, with identical chemical shifts—for example the protons in CH₄ or the fluorines in CF₃COOH. This somewhat loose definition will be refined at the end of this section.

The following paragraphs deal with the effect of spins M and X on the NMR signal of spin A. The convention is that spins with very different chemical shifts are labelled by letters far apart in the alphabet (e.g. A, M, X). Nuclei having similar shifts, and thus likely to be strongly coupled, are assigned adjacent letters in the alphabet (e.g. A, B, C).

Finally it must be said that the predictions in the following paragraphs are not infallible: the expected multiplet patterns may be obscured if the splitting is smaller than the linewidth (see Chapter 5), or modified if the molecule is undergoing a dynamic process that causes the *J*-couplings to be time-dependent (see Chapter 4).

Coupling to a single spin-1/2 nucleus (AX)

As already discussed for $H^{13}CO_2^-$, the interaction of nucleus A with a single spin- $\frac{1}{2}$ nucleus, X, causes the A resonance to split into two equally intense lines centred at the chemical shift of A (a doublet), with spacing equal to the AX coupling constant, J_{AX} . The interaction is symmetrical, so that the spectrum of X is also a doublet, with the same splitting (Figs 3.2–3.4).

Coupling to two inequivalent spin-1/2 nuclei (AMX)

The next level of complexity is the AMX spin system, which consists of three nuclei with different chemical shifts and three distinct coupling constants: J_{AM} , J_{AX} , J_{MX} . Equation 3.2 can be used to predict the spectrum of A, by drawing up a list of the possible values of the magnetic quantum numbers of M and X (Table 3.1). Four lines are expected because there are four non-degenerate arrangements of the

m _M	m _X	$\sum_{K=M,X} J_{AK} m_{K}$
+ 1/2	+ 1/2	$+\frac{1}{2}(J_{AM}+J_{AX})$
+ 1/2	$-\frac{1}{2}$	$+\frac{1}{2}(J_{AM}-J_{AX})$
$-\frac{1}{2}$	+ 1/2	$-\frac{1}{2}(J_{AM}-J_{AX})$
$-\frac{1}{2}$	$-\frac{1}{2}$	$-\frac{1}{2}(J_{AM}+J_{AX})$

Table 3.1 Spin-spin coupling in an AMX spin system

The final column gives the shift in the Larmor frequency of A for each of the four spin configurations of M and X (both $I = \frac{1}{2}$) (see eqn 3.2).

M and X spins (M \uparrow X \uparrow , M \uparrow X \downarrow , M \downarrow X \uparrow , M \downarrow X \downarrow). These peaks are displaced from the chemical shift of A by simple combinations of J_{AM} and J_{AX} (but not J_{MX}). The A multiplet should therefore be a *doublet of doublets*, as shown in Fig. 3.5(a).

A different way to see how this pattern arises is to construct the spectrum in stages using the 'tree diagram 'approach shown in Fig. 3.5(a). Imagine first of all that both J_{AM} and J_{AX} are zero, so that the spectrum of A is a singlet at the chemical shift position. Now suppose the AM coupling is 'switched on', to give a doublet with splitting J_{AM} . Finally, when the AX coupling is introduced, each of the lines of the doublet is itself split into a doublet, with splitting JAX. This stepwise procedure is probably the quickest way of arriving at multiplet patterns. The order in which the couplings are introduced is irrelevant. Of course, the exact appearance of the doublet of doublets will depend on the values (but not the signs) of the coupling constants. This point is illustrated later (Fig. 3.13) for a four-spin system.

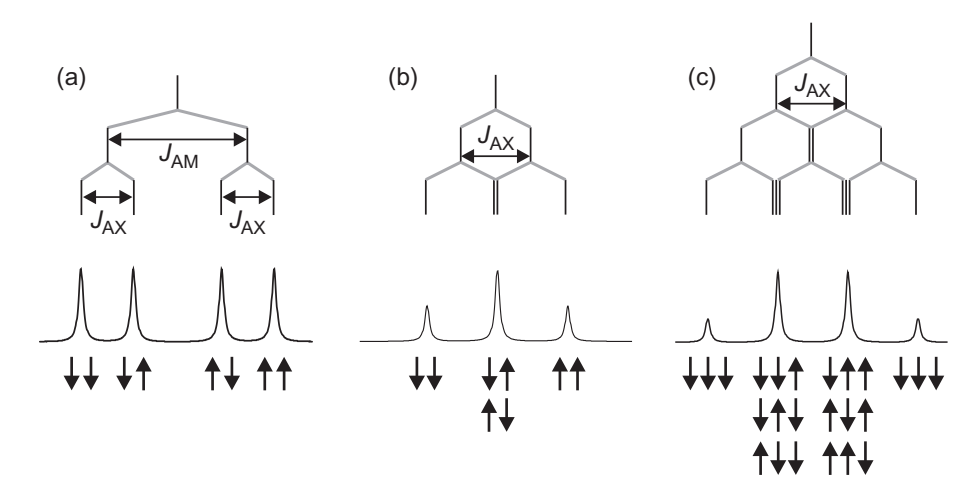


Fig. 3.5 (a) The NMR spectrum of nucleus A in an AMX spin system. The four components of the A multiplet, a doublet of doublets, arise from the four combinations of M and X magnetic quantum numbers, indicated $\uparrow (m=+\frac{1}{2})$ and $\downarrow (m=-\frac{1}{2})$. (b) The spectrum of nucleus A in an AX₂ spin system. (c) The spectrum of nucleus A in an AX₃ spin system. The spectra are drawn for $J_{AM} > J_{AX} > 0$. The tree diagrams above the spectra show how the multiplet patterns arise.

29

Coupling to two equivalent spin-½ nuclei (AX₂)

This is a special case of the AMX spin system, with $J_{AM}=J_{AX}$. As may be seen from Table 3.1 and Fig. 3.5(b), the two central lines of the doublet of doublets coincide so that the multiplet becomes a *triplet* centred at the chemical shift of A, with line-spacing equal to the coupling constant, and relative intensities 1:2:1. The central line of the triplet arises from two degenerate arrangements of the X spins ($\uparrow \downarrow$ and $\downarrow \uparrow$), in both of which the local magnetic fields due to the X nuclei exactly cancel.

Coupling to three equivalent spin-1/2 nuclei (AX3)

The multiplet pattern of A in an AX₃ spin system (three identical AX coupling constants) is a four-line quartet (Fig. 3.5(c) and Table 3.2). There are two peaks displaced from the chemical shift position by $\pm \frac{3}{2}J_{AX}$ and two peaks with three times the intensity at $\pm \frac{1}{2}J_{AX}$. The inner lines, for example, have relative intensity 3 because there are three degenerate ways of achieving a total magnetic quantum number of $\pm \frac{1}{2}$.

Coupling to n equivalent spin- $\frac{1}{2}$ nuclei (AX_n)

It should be clear how the results for AX, AX_2 , and AX_3 can be generalized. For n equivalent X nuclei, the A resonance is split into n + 1 equally spaced lines, with

Table 3.2 Spin-spin coupling in an AX₃ spin system

<i>m</i> ₁	m ₂	<i>m</i> ₃	$\sum_{i=1,2,3} J_{AX} m_i$
$+\frac{1}{2}$	+ 1/2	+ 1/2	$+\frac{3}{2}J_{AX}$
$+\frac{1}{2}$	+1/2	$-\frac{1}{2}$	
+ 1/2	$-\frac{1}{2}$	+ 1/2	$\left.\begin{array}{l} +\frac{1}{2}J_{AX} \end{array}\right.$
$-\frac{1}{2}$	+ 1/2	+ 1/2	
+ 1/2	$-\frac{1}{2}$	$-\frac{1}{2}$	
$-\frac{1}{2}$	+1/2	$-\frac{1}{2}$	$\left\frac{1}{2}J_{AX} \right.$
$-\frac{1}{2}$	$-\frac{1}{2}$	+ 1/2	J
$-\frac{1}{2}$	$-\frac{1}{2}$	$-\frac{1}{2}$	$-\frac{3}{2}J_{AX}$

The final column shows the shift in the Larmor frequency of A for each of the eight spin configurations of the three X spins $(I = \frac{1}{2})$, labelled 1, 2 and 3 (see eqn 3.2).

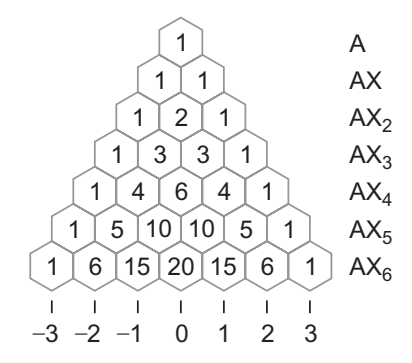


Fig. 3.6 Pascal's triangle showing the binomial coefficients in the expansion of $(1+x)^n$. The rows give the relative intensities of the n+1 lines in the A multiplet of an AX_n spin system (n=0-6), where X is a spin- $\frac{1}{2}$ nucleus. As indicated at the bottom of the figure, the columns give the positions of the lines relative to the chemical shift position, in units of J_{AX} .

relative intensities given by simple combinatorial arithmetic. The amplitude of the m-th line ($m = 0, 1, 2, \dots n$) of an AX_n multiplet is simply the number of ways in which m spins can be \uparrow and (n - m) spins \downarrow , i.e. n!/m!(n - m)!. To put it another way, the amplitudes are given by the coefficients in the binomial expansion of $(1 + x)^n$, or, equivalently by the (n + 1)-th row of Pascal's triangle (Fig. 3.6).

Coupling involving *I* > ½ nuclei

If the nucleus of interest, A, has spin quantum number greater than $\frac{1}{2}$, its multiplet structure can be predicted in exactly the same way as for a spin- $\frac{1}{2}$ nucleus. This can be seen from eqns 3.1 and 3.2, and is demonstrated in Fig. 3.7 for a spin-1 coupled to a spin- $\frac{1}{2}$. For example, the ¹⁴N (I=1) and ¹⁵N ($I=\frac{1}{2}$) NMR spectra of, respectively, ¹⁴NH⁴ and ¹⁵NH⁴ both consist of a quintet, with relative peak

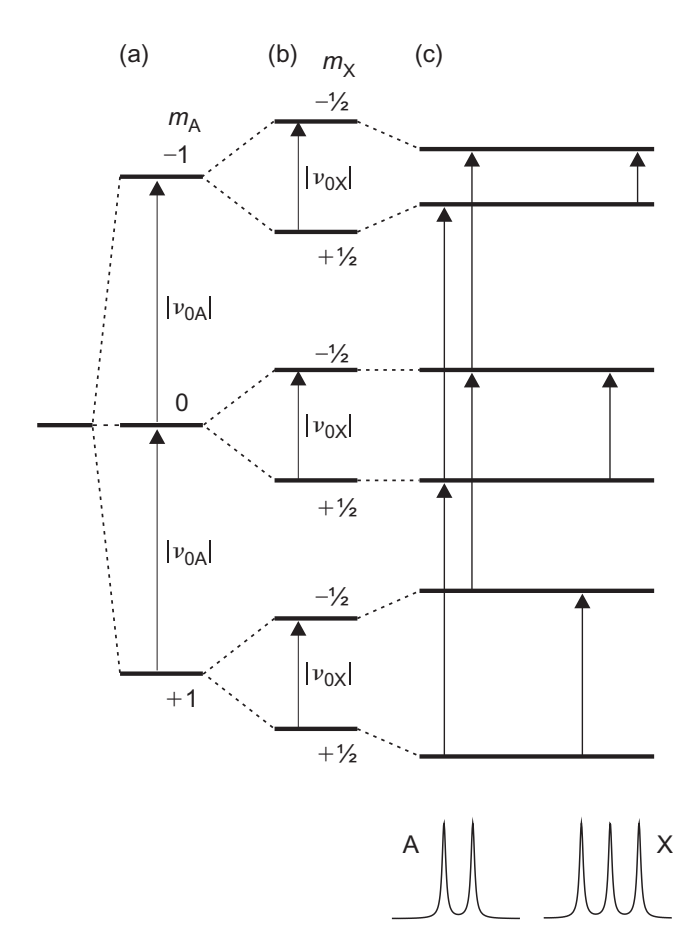


Fig. 3.7 Energy levels and spectra of a spin-1 nucleus (A) coupled to a spin- $\frac{1}{2}$ nucleus (X). From left to right, magnetic interactions are introduced in the order: (a) the interaction of A with the magnetic field B_0 ; (b) the interaction of X with B_0 ; (c) the spin-spin coupling, $J = J_{AX}$. The spectrum of A is a doublet because its four allowed NMR transitions are pairwise degenerate. The spectrum of X comprises three lines arising from the m = +1, 0, -1 states of A. For clarity, the energy-level shifts are not drawn to scale. v_{0A} and v_{0X} are the Larmor frequencies of the two spins in the absence of coupling. The shifts in the energy levels are given as frequencies. The figure is drawn for $\gamma_A > 0$, $\gamma_X > 0$ (so that v_{0A} and v_{0X} are both negative) and $J_{AX} < 0$. The energy levels are labelled with the appropriate magnetic quantum numbers.

intensities 1:4:6:4:1. The NH coupling constants of the two isotopologues are in the ratio 0.713:1, which is the ratio of the magnetogyric ratios of the two nitrogen isotopes (see Table 1.3).

However, nuclei with $I > \frac{1}{2}$ possess, in addition to their magnetic dipole moment, an *electric quadrupole moment* that can interact with local *electric field gradients*. For molecules tumbling in solution, this interaction can lead to efficient relaxation of the quadrupolar nucleus giving NMR lines that may be so broad that the expected multiplet patterns are partially or completely obscured. This quadrupolar relaxation mechanism is discussed further in Section 5.7.

For A $(I=\frac{1}{2})$ coupled to X $(I>\frac{1}{2})$, the principles established above for spin- $\frac{1}{2}$ nuclei can easily be extended. A spin-I particle has energy levels corresponding to 2I+1 orientations of its magnetic moment with respect to the magnetic field B_0 . Therefore, a nucleus coupled to a single X spin with quantum number I should show a multiplet comprising 2I+1 lines with equal spacings and amplitudes. For example, the 13 C spectrum of deuterated chloroform, 13 CDCl₃, is a 1:1:1 triplet arising from the three equally probable states of the deuteron, m=+1, 0, -1 (Fig. 3.7). Once again, quadrupolar relaxation may upset these predictions. Rapid relaxation of the quadrupolar nucleus may have the effect of 'decoupling 'A and X, such that no splitting is observed in the spectrum of A. For example, 35 Cl and 37 Cl (both $I=\frac{3}{2}$) rarely produce splittings in the NMR spectra of nearby nuclei. We shall return to this point in Section 5.7.

For coupling to *equivalent I* > $\frac{1}{2}$ nuclei, the multiplet patterns are easily deduced using the 'tree diagram 'approach introduced in Fig. 3.5. For instance, the terminal protons of $^{11}B_2H_6$ (diborane) show a 1:1:1:1 quartet due to coupling to the directly bonded ^{11}B ($I=\frac{3}{2}$), while the bridge protons exhibit a seven-line pattern with relative intensities 1:2:3:4:3:2:1, arising from equal interactions with the two symmetrically placed borons (Fig. 3.8).

Equivalent nuclei

Up to now, we have used the term *equivalent* somewhat loosely to describe nuclei with identical chemical shifts, usually as a result of molecular symmetry. In fact there are two kinds of equivalence: *chemical* and *magnetic*. The distinction is

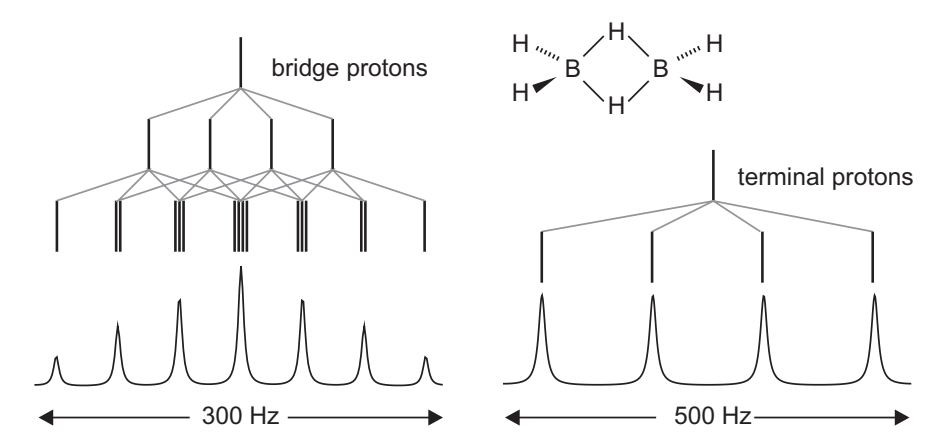


Fig. 3.8 ¹H NMR spectra of the terminal and bridge protons in diborane, ¹¹B₂H₆.

The term 'tumbling 'denotes the rapid chaotic rotational motion of a molecule in a liquid. Collisions with other molecules cause frequent changes in the axis and rate of rotation.

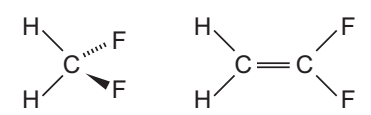


Fig. 3.9 CH₂F₂ (magnetically equivalent protons) and CH₂=CF₂ (chemically equivalent protons).

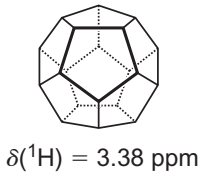


Fig. 3.10 Dodecahedrane, ¹²C₂₀H₂₀. The 20 protons are magnetically equivalent.

best seen by means of an example. Consider the protons in the two compounds CH_2F_2 and $CH_2=CF_2$ (Fig. 3.9). In CH_2F_2 , the two protons have the same chemical shift *and* each has identical couplings to each of the fluorines: as such they are termed *magnetically equivalent*. The same cannot be said of $CH_2=CF_2$, where the *cis* and *trans* $^1H_2^{-19}F$ coupling constants differ: in this case the protons are said to be *chemically equivalent*.

More generally, a set of nuclei (a, b, c, \ldots) with identical chemical shifts are magnetically equivalent *either* if there are no other spins in the molecule *or* if, for every other nucleus (e.g. z) in the molecule, the spin-spin coupling constants satisfy the relation

$$J_{az} = J_{bz} = J_{cz} = \cdots (3.3)$$

As might be expected, the NMR spectra of molecules containing chemically equivalent spins are rather more complex than for similar compounds with magnetically equivalent nuclei. For example, the 1H spectrum of $CH_2=CF_2$ has no fewer than ten lines. The analysis of such spectra is not straightforward and will not be attempted here: a good discussion is given by Günther (2013). In the remainder of this section we concentrate on magnetically equivalent spins.

The ${}^{1}\text{H}$ spectrum of $\text{CH}_{2}\text{F}_{2}$ comprises just three lines: a 1:2:1 triplet with splitting equal to the proton-fluorine coupling constant $J_{\text{HF}}({}^{19}\text{F}\text{ is spin}-\frac{1}{2})$. The remarkable thing about this spectrum is not the triplet, which is exactly what one would expect for a *single* proton coupled to two identical fluorines, but the *absence* of any splittings arising from the ${}^{1}\text{H}-{}^{1}\text{H}$ coupling. Although the two protons interact (they are only two bonds apart), their mutual coupling is not manifest as a splitting in the spectrum. This is a general feature of J-coupling: spin-spin interactions within a group of magnetically equivalent nuclei do not produce multiplet splittings.

Perhaps without realizing it, we have already seen several instances of this phenomenon: each of the five molecules in Fig. 2.6 contains a single group of (magnetically) equivalent protons and each gives rise to an NMR singlet. A more esoteric example is the highly symmetrical molecule dodecahedrane (Fig. 3.10) whose ¹H spectrum also consists of a single peak.

The high resolution spectrum of ethanol in Fig. 3.1 can now be understood. The ethyl protons make up an A_3X_2 spin system: the triplet arises because each of the CH_3 protons couples equally to the two equivalent CH_2 protons, while the quartet comes from the CH_2 protons interacting identically with each of the CH_3 protons. As discussed in Chapter 4, rapid internal rotation around the C-C bond averages out the chemical shift differences associated with the different conformations of the molecule, and effectively renders the three methyl protons magnetically equivalent to one another, and similarly the two methylene protons. The absence of splittings from coupling between the CH_2 group and the OH proton is another story, also told in Chapter 4.

In Section 3.5, we shall see *why* magnetically equivalent nuclei do not split one another's NMR lines, but first a few examples that illustrate how multiplet patterns can be used to determine or verify the structures of molecules without prior knowledge of the magnitudes of the chemical shifts or coupling constants involved.

3.4 Examples

Fig. 3.11 shows the very different ³¹P NMR spectra of three closely related phosphorus–sulphur compounds: $\alpha P_4 S_4$, $\beta P_4 S_4$, and $\beta P_4 S_5$. The multiplet structure arises entirely from ³¹P–³¹P couplings because ³²S, the only isotope of sulphur with an appreciable natural abundance (99.24%), has spin I=0. The three spin systems A_4 ($\alpha P_4 S_4$), AMX_2 ($\beta P_4 S_4$), and $A_2 X_2$ ($\beta P_4 S_5$) are easily deduced from the spectra, and are clearly consistent with the structures shown.

The tetrameric structure of t-butyl lithium is clearly revealed by low temperature 13 C and 7 Li NMR (Fig. 3.12). The 7 Li spectrum of 7 Li 13 CMe $_{3}$ consists of a 1:3:3:1 quartet: each lithium interacts with three equivalent t-butyl carbons, and has an unresolved (i.e. very small) coupling to the fourth, more distant 13 C. Similarly, the 13 C spectrum of 6 Li 13 CMe $_{3}$ is a septet, with relative intensities 1:3:6:7:6:3:1, produced by each of the four equivalent 13 C spins interacting with three equivalent I = 1 6 Li nuclei. The two coupling constants, $J(^{7}$ Li 13 C) = 14.3 Hz and $J(^{6}$ Li 13 C) = 5.4 Hz, are in the ratio of the magnetogyric ratios of the two Li isotopes (1.04 × 108 and 3.94 × 107 T $^{-1}$ s $^{-1}$ respectively). As discussed in Chapter 4, these spectra are modified at higher temperatures by rapid rearrangement of the t-butyl groups.

A slightly more complex case is the 1 H spectrum of 1,3-bromonitrobenzene, Fig. 3.13. This is a weakly coupled AMPX spin system with all six pairwise couplings resolved, so that each proton gives a doublet of doublets of doublets, i.e. eight lines. The exact appearance of each multiplet is determined by the magnitudes of the coupling constants, and may readily be understood by noting that $|J_{ortho}| > |J_{meta}| > |J_{para}|$. For the A and X multiplets, the central pair of lines overlap strongly and appear as a single line of double intensity. Two further illustrations of the use of spin-spin couplings in structural studies are given in Chapter 6 (Figs 6.18 and 6.19).

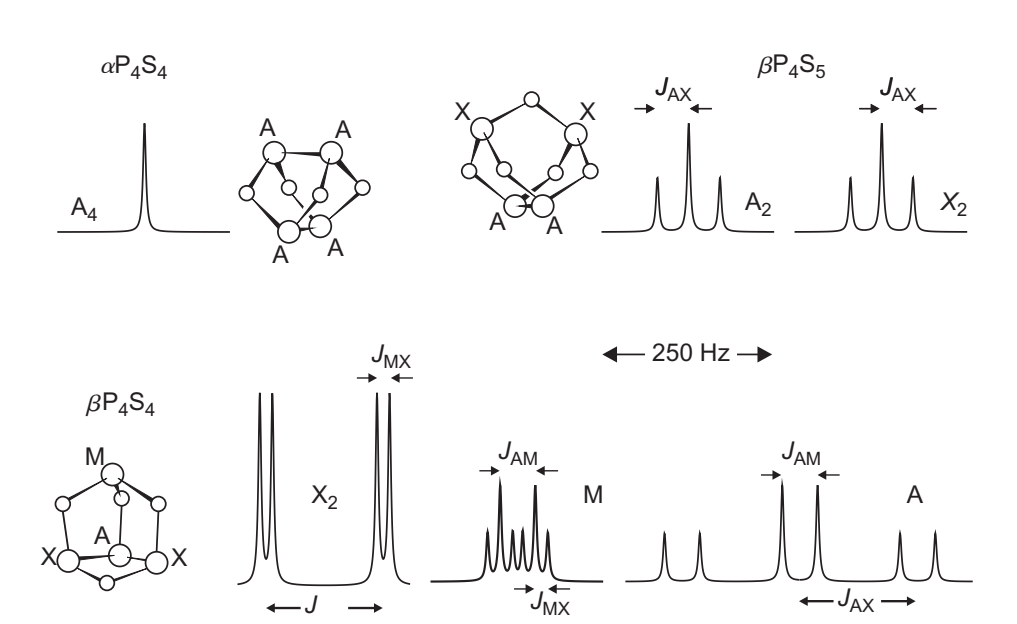
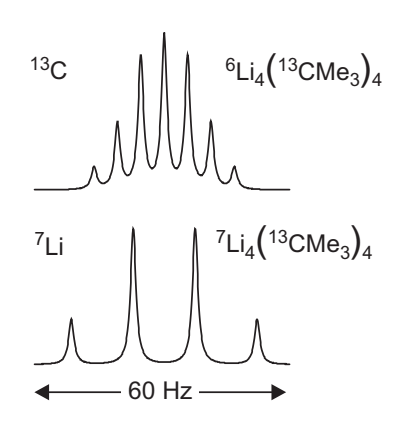


Fig. 3.11 ³¹P NMR multiplets of $\alpha P_4 S_4$, $\beta P_4 S_4$, and $\beta P_4 S_5$. The larger spheres represent the phosphorus atoms.



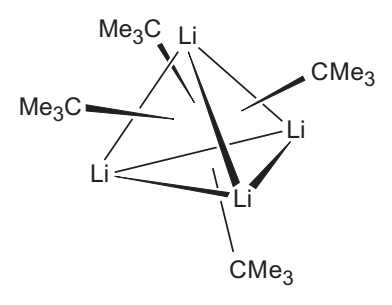


Fig. 3.12 ^{13}C spectrum of $^{6}\text{Li}_{4}(^{13}\text{CMe}_{3})_{4}$ and ^{7}Li spectrum of $^{7}\text{Li}_{4}(^{13}\text{CMe}_{3})_{4}$. Both spectra were recorded using ^{1}H -decoupling to remove the multiplet splittings caused by the ^{1}H nuclei.

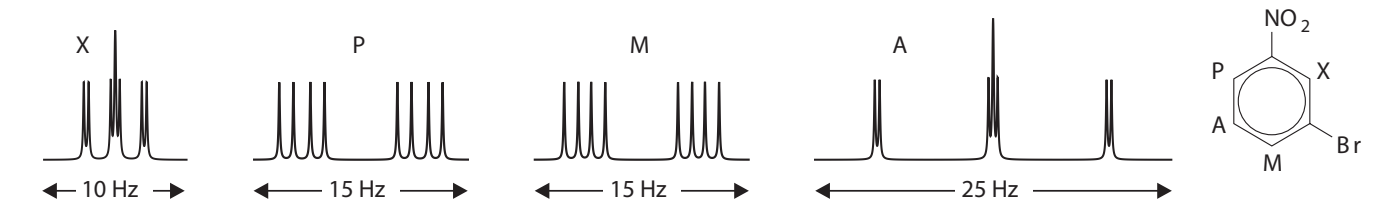


Fig. 3.13 1 H NMR spectrum of 1,3-bromonitrobenzene. The six coupling constants are: $J_{AM} = 7.98$ Hz; $J_{AP} = 8.28$ Hz; $J_{MP} = 0.99$ Hz; $J_{MX} = 1.89$ Hz, $J_{PX} = 2.18$ Hz, $J_{AX} = 0.34$ Hz.

¹³C NMR

As an NMR nucleus, 13 C is second in popularity only to 1 H: it is therefore appropriate at this point to comment briefly on multiplet splittings in 13 C spectra. In organic molecules, the dominant couplings experienced by 13 C nuclei are with their directly bonded protons. One-bond C–H coupling constants generally fall in the range 100-250 Hz, and are often an order of magnitude larger than two-bond and three-bond C-H interactions. The 13 C multiplets produced by one-bond couplings—a quartet for a methyl carbon (CH₃), a triplet for a methylene (CH $_2$), a doublet for a methine (CH), and a singlet for a quaternary carbon (C)—provide valuable clues when attempting to assign peaks in a spectrum to particular carbons in the molecule. However, 13 C NMR spectra are normally measured with the protons decoupledso as to remove the 13 C– 1 H splittings. This is achieved by irradiating the sample at the 1 H resonance frequency (about four times that of 13 C) while the 13 C spectrum is being recorded. The result is a considerably simplified spectrum: in the absence of heteronuclei (19 F, 31 P, etc.) each inequivalent carbon site in a molecule gives rise to a singlet in the 1 H-decoupled 13 C spectrum (denoted 13 C 1 H 1).

Not only are ¹³C{¹H} spectra less crowded than those with the proton–carbon couplings present, they also have higher sensitivity. The latter arises from the nuclear Overhauser enhancement (a relaxation phenomenon described in Section 5.5) and because all the NMR intensity for each multiplet is concentrated into a single line.

Finally, homonuclear ($^{13}C-^{13}C$) couplings are not normally observed in ^{13}C spectra because of the low natural abundance of ^{13}C (1.1%). Taking ethanol as an example, it is clear that of the molecules containing a ^{13}C at a given position, only about 1 in 100 contains a second ^{13}C . Thus, the spectrum of $^{13}CH_3^{13}CH_2OH$ should be about 100 times weaker than that of either $^{12}CH_3^{13}CH_2OH$ or $^{13}CH_3^{12}CH_2OH$. $^{13}C-^{13}C$ splittings therefore often go unnoticed. Of course $^{12}CH_3^{12}CH_2OH$, by far the most abundant isotopologue, has no ^{13}C NMR spectrum at all. For more on ^{13}C NMR see Wehrli et al. (1988), Friebolin (2011), and Günther (2013).

3.5 Strong coupling and equivalent spins

In Sections 3.2–3.4 we saw that the spectrum of a pair of coupled spin- $\frac{1}{2}$ nuclei can either be two doublets (weak coupling) or one singlet (magnetic equivalence). To shed some light on this, and on what happens between these two

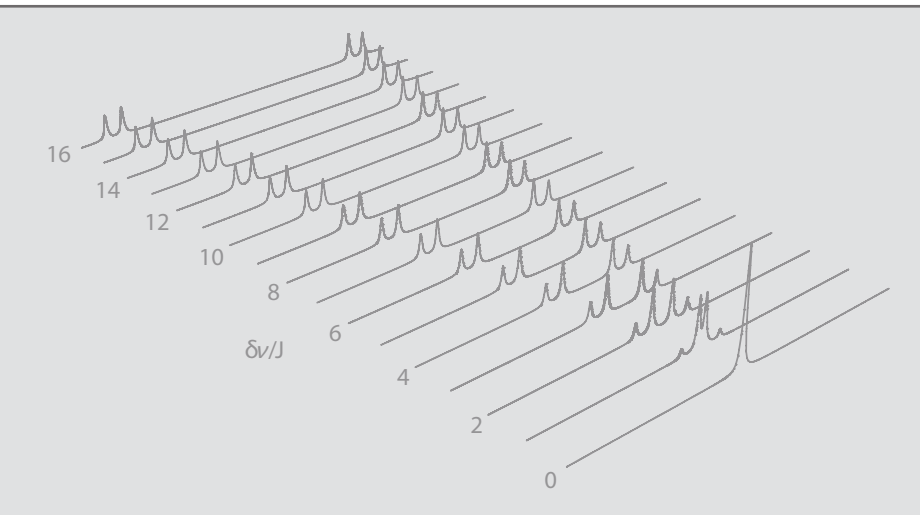


Fig. 3.14 Calculated NMR spectra of a pair of spin- $\frac{1}{2}$ nuclei for fixed Jand a range of values of δv .

extremes, we start with Fig. 3.14 which shows spectra calculated for a range of values of $\delta v = v_{0A} - v_{0B}$ (the difference in chemical shift frequencies of spins A and B). Keeping the J-coupling fixed, the two doublets move together as their chemical shifts become more similar. At the same time, the inner components of the four-line pattern steadily become stronger while the outer components become weaker. Eventually, when $\delta v = 0$, the inner lines coincide and the outer lines vanish.

We denote the $m = +\frac{1}{2}$ and $m = -\frac{1}{2}$ states of each spin α and β respectively, so that the four states of the weakly coupled pair are

$$\alpha_A \alpha_B$$
, $\alpha_A \beta_B$, $\beta_A \alpha_B$, $\beta_A \beta_B$.

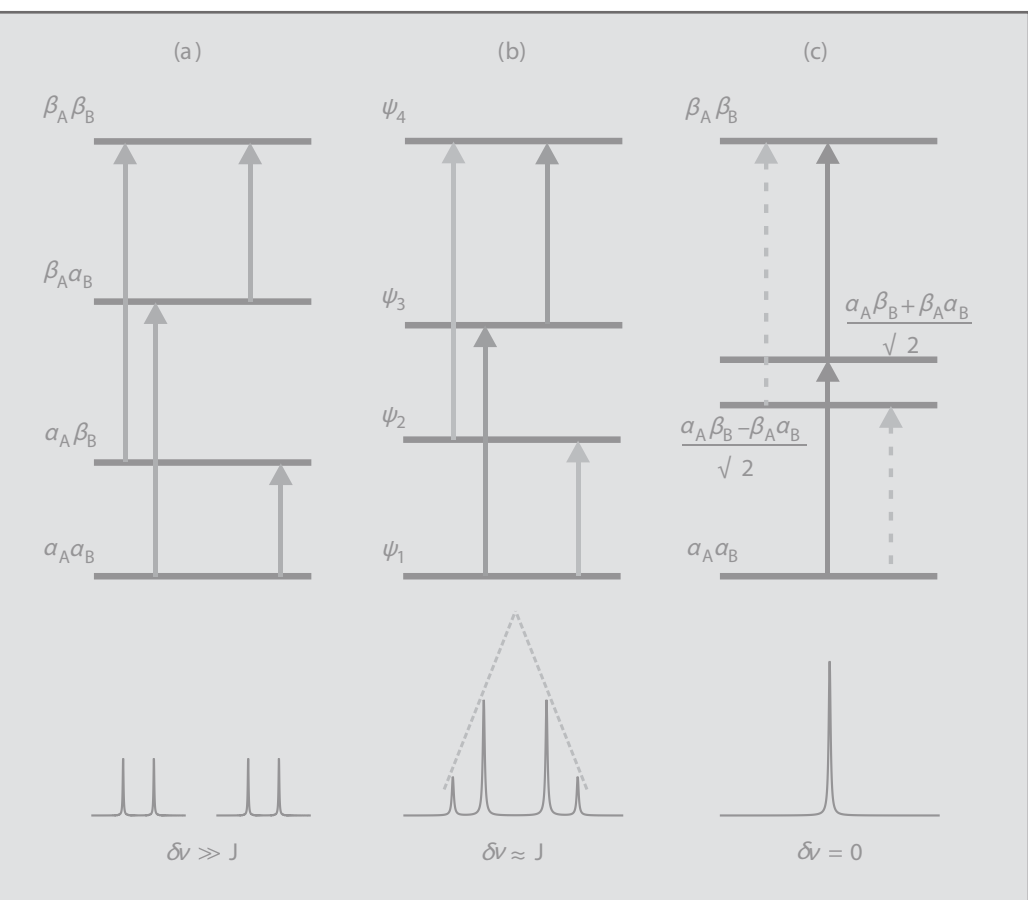
As described in Section 3.2, the four allowed transitions,

$$\alpha_A \alpha_B$$
 $\alpha_A \beta_B$, $\alpha_A \alpha_B$ $\beta_A \alpha_B$, $\alpha_A \beta_B$ $\beta_A \beta_B$, $\beta_A \alpha_B$ $\beta_A \beta_B$,

have distinct frequencies and equal intensities giving the familiar pair of doublets (Fig. 3.15(a)). As δv becomes smaller, the separation of the two central states becomes comparable to Jwith the result that they mix. Instead of being pure $\alpha_A\beta_B$ and $\beta_A\alpha_B$ they become linear combinations of $\alpha_A\beta_B$ and $\beta_A\alpha_B$. The consequence is a change in the transition probabilities and transition frequencies The inner lines become more allowed (i.e. stronger) and the outer pair less allowed (weaker), the effect being more pronounced as $\delta v/J$ becomes smaller (Fig. 3.15(b)). In the limit $\delta v = 0$, the outer lines are forbidden and the inner lines have the same frequency (Fig. 3.15(c)).

To make this more concrete, we now summarize the results of a quantum mechanical treatment (Hore, Jones & Wimperis (2015)). The four states ψ_j and their energies E_i are:

$$\begin{split} \psi_{1} &= \alpha_{A} \alpha_{B} & E_{1} / h = + \nu + \frac{1}{4} J \\ \psi_{2} &= \cos \chi \, \alpha_{A} \beta_{B} + \sin \chi \, \beta_{A} \alpha_{B} & E_{2} / h = + \frac{1}{2} C - \frac{1}{4} J \\ \psi_{3} &= -\sin \chi \, \alpha_{A} \beta_{B} + \cos \chi \, \beta_{A} \alpha_{B} & E_{3} / h = -\frac{1}{2} C - \frac{1}{4} J \\ \psi_{4} &= \beta_{A} \beta_{B} & E_{4} / h = - \nu + \frac{1}{4} J \end{split} \tag{3.4}$$



We assume that $\delta v > 0$ and J > 0 to avoid the use of moduli, e.g. $|\delta v| \gg |J|$.

Fig. 3.15 Energy levels and spectra of a pair of spin- $\frac{1}{2}$ nuclei, A and B. (a) weak coupling ($\delta v \gg J$), (b) strong coupling ($\delta v \approx J$), and (c) equivalent spins ($\delta v = 0$). Dashed arrows: forbidden transitions. Solid arrows: the darker the arrow, the higher the transition probability and the stronger the corresponding NMR line.

where

$$v = \frac{1}{2} (v_{0A} + v_{0B}), C = \sqrt{J^2 + (\delta v)^2}, \tan 2\chi = \frac{J}{\delta v}$$
 (3.5)

As noted above, ψ_2 and ψ_3 are linear combinations of $\alpha_A\beta_B$ and $\beta_A\alpha_B$ and have energies that depend on the strength of the coupling $\psi(\delta v)$, specified by the angle χ . ψ_1 and ψ_4 , being well separated in energy from each other and from ψ_2 and ψ_3 , are independent of the coupling strength.

Table 3.3 summarizes the frequencies of the four lines, $(E_j-E_k)/h$, and their relative intensities. In the weak coupling limit $(\delta v\gg J)$ it can be seen from eqn 3.5 that $C\approx\delta v$ and $\chi\approx0$ so that the four lines all have relative intensity 1 and occur at the expected frequencies: $v0A\pm12J$ and $v0B\pm12J$. In the other extreme (equivalent spins), C=J and $\chi=45^\circ$ so that the line positions are v-J, v, v, v+J with relative intensities 0, 2, 2, 0 respectively.

The spectra in Fig. 3.15 are generally given the names AX (weak coupling), AB (strong coupling), and A_2 (equivalent spins). The intensity distortions arising from strong coupling are sometimes referred to as the 'roof effect '(indicated by the sloping dashed lines above the spectrum in Fig. 3.15(b)). In the presence of strong coupling, the doublets still have splitting equal to but they are no longer centred at the chemical shift positions.

37

Table 3.3 Frequencies and relative intensities of the NMR lines of a strongly coupled pair of $I = \frac{1}{2}$ spins

transition	frequency	relative intensity ^a
3 4	$v - \frac{1}{2}C - \frac{1}{2}J$	$1-\frac{J}{C}$
1 2	$V - \frac{1}{2}C + \frac{1}{2}J$	$1+\frac{J}{C}$
2 4	$v + \frac{1}{2}C - \frac{1}{2}J$	1+ <mark>J</mark>
1 3	$v + \frac{1}{2}C + \frac{1}{2}J$	$1-\frac{J}{C}$

^a When J>0, transitions 3 4 and 1 3 are the outer (weaker) lines of each doublet and 1 2 and 2 4 are the inner (stronger) lines. *v* and C are defined in eqn 3.5.

Closer inspection of egn 3.4 gives a little more insight into the absence of splittings in the spectra of magnetically equivalent spins. The four states in eqn 3.4 can be classified according to their symmetry with respect to interchange of the A and B labels. When $\delta v = 0$, $\psi_3 = 2^{-1/2} (\beta_A \alpha_B - \alpha_A \beta_B)$ and is antisymmetric (a singlet state). In the same limit, $\psi_1 = \alpha_A \alpha_B$, $\psi_2 = 2^{-1/2} (\alpha_A \beta_B + \beta_A \alpha_B)$ and $\psi_4 = \beta_A \beta_B$, are all symmetric(triplet state); unlike ψ_3 they do not change sign when the spin labels are exchanged. The three triplet energy levels are equally spaced (Fig. 3.15(c)) and can be thought of as arising from a 'compound 'nucleus with I = 1. Similarly, the singlet energy level can be regarded as coming from a non-magnetic nucleus (I = 0). Looked at in this way, the spectrum of two equivalent spins is simply that of an isolated spin-1 nucleus, i.e. a single line at the chemical shift. Put another way, the two transitions involving the triplet energy levels, ψ_1 ψ_2 ψ_4 , are allowed and degenerate, while the singlet-triplet transitions, ψ_1 ψ_3 ψ_4 , which would have frequencies $\pm J$ either side of the chemical shift position, are completely forbidden and have zero intensity (Fig. 3.15(c)).

As one might anticipate, the effects of strong coupling can be much more complicated when more than two spins are involved. The multiplet patterns discussed in Section 3.3 can be so severely distorted that they become difficult to recognize; the changes in transition probabilities cause otherwise forbidden transitions to be observed, and chemical shifts and coupling constants can no longer be extracted without a detailed analysis. Such problems are alleviated by the use of high-field spectrometers. Because coupling constants are independent of B_0 and $\delta \nu$ is proportional to B_0 (eqn 2.3), a strongly coupled spin system often becomes weakly coupled at higher field. For example, a pair of protons with J=6 Hz and chemical shift difference of 0.2 ppm would show a pronounced roof effect on a 60 MHz spectrometer ($J/\delta \nu=0.5$) but not at 600 MHz ($J/\delta \nu=0.5$).

For discussions of strong coupling effects in larger spin systems, see Bovey (1988) and Günther (2013).

3.6 Mechanism of spin-spin coupling

So far, nothing has been said about the *origin* of spin-spin coupling, apart from some vague statements about nuclei being the source of local magnetic fields that affect the energies of other nuclei. The most obvious interaction between two nearby spins is their mutual *dipolar* coupling (Appendix A). In roughly the same way that two bar magnets interact, so pairs of neighbouring nuclei sense one another's orientation through their dipolar magnetic fields. However, as outlined in Section 3.8, this anisotropic interaction averages to zero for molecules tumbling rapidly and isotropically in solution, and so cannot be responsible for the multiplets discussed in Section 3.3.

The principal source of *J*-coupling in molecules is an *indirect* interaction mediated by the valence electrons.

Contact interaction

We start by considering an electron spin interacting with a nuclear spin. The electron has spin- $\frac{1}{2}$ and a magnetogyric ratio some 660 times that of a proton. Unpaired electrons therefore have strong magnetic dipolar interactions with nearby nuclei but, being purely anisotropic, they should average to zero for molecules tumbling in solution. This indeed happens, *except* at electron–nuclear separations comparable to the nuclear radius (~ 10^{-14} m) where the particles can no longer be thought of as point dipoles. This breakdown of the point–dipole approximation can be visualized by thinking of the nucleus as a circular current loop of radius ~ 10^{-14} m. Far from the centre of the loop, the field it generates indeed has a $3\cos^2\theta - 1$ dependence (see Section 3.8), but *inside* the loop, the magnetic flux lines are nearly parallel, with little angular variation (see, e.g., Fig. 2.24).

In fact, at very small separations, the dipolar interaction of an electron and a nucleus is replaced by an *isotropic* coupling known as the Fermi *contact interaction*. Its strength is proportional to the scalar product of the two magnetic moments

contact interaction
$$\propto -\gamma_e \gamma_n I$$
. (3.6)

where ${\bf I}$ and ${\bf S}$ are respectively the nuclear and electron spin angular momentum vectors. Since the electron has a *negative* magnetogyric ratio ($\gamma_e < 0$), a nucleus with $\gamma_n > 0$ is *stabilized* if the electron and nuclear spins are *antiparallel* (${\bf I} \cdot {\bf S} < 0$), and *destabilized* if they are *parallel* (${\bf I} \cdot {\bf S} > 0$), Fig. 3.16. The magnitude of the interaction is also proportional to the probability of finding the electron at the nucleus (R = 0) and therefore vanishes unless the electronic wavefunction has some s-electron character (p, d, f, etc. wavefunctions have no amplitude at R = 0). In short, this isotropic interaction allows an electron spin to sense the state of a nearby nuclear spin, in a way that survives the orientational averaging effect of rapid molecular tumbling.

In paramagnetic atoms and molecules (i.e. those with one or more unpaired electrons), the contact interaction produces *hyperfine* splittings of lines in electronic spectra and electron spin resonance spectra. More importantly in the present context, it provides a pathway for spin-spin coupling between *pairs of nuclei*.

The averaging of dipolar interactions by molecular tumbling is discussed in Sections 3.8 and 5.6.

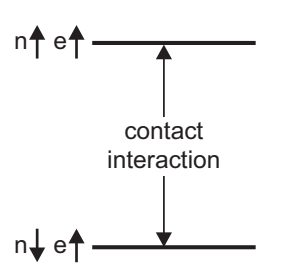


Fig. 3.16 Energy levels of an electron, e, and a spin- $\frac{1}{2}$ nucleus, n ($\gamma_n > 0$), with a Fermi contact interaction. The antiparallel configuration of spins is stabilized relative to the parallel arrangement.

Indirect coupling between nuclei

At first sight it seems unlikely that the contact interaction could form the basis of a general mechanism of nuclear *J*-coupling. Most molecules have closed electronic shells with no unpaired electrons and therefore, one might think, no contact interactions.

To get an idea of how spin-spin coupling comes about, consider the simplest diamagnetic molecule, H_2 . Ignoring normalization constants, the ground state electronic wavefunction may be written

$$\Psi_0 = \phi_0 (\alpha_a \beta_b - \beta_a \alpha_b) \tag{3.7}$$

 Ψ_0 has two parts: the spatial wavefunction ϕ_0 (the molecular orbital) and the electron-spin function. The two electron spins, a and b, are paired (i.e. a singlet state) in a bonding orbital formed from the two atomic 1s orbitals (Fig. 3.17(a)). As before, α and β are shorthand for $m=+\frac{1}{2}$ and $m=-\frac{1}{2}$ respectively. From the form of Ψ_0 and the Born interpretation of the wavefunction, it is clear that the spatial distributions of the α and β states of both electrons are identical and given by $|\phi_0|^2$.

The contact interaction mixes the singlet ground state with electronically excited triplet states of the molecule. Crudely speaking, this happens because the nucleus–electron coupling can flip the spin of one of the electrons, converting singlet (antiparallel spins) to triplet (parallel spins), while simultaneously flipping the nuclear spin in the opposite sense so as to conserve angular momentum. The singlet \rightarrow triplet mixing must be accompanied by electronic excitation because the Pauli principle forbids two electrons with parallel spins to be in the same orbital. In the case of H_2 , the lowest excited triplet state is accessed by promoting one of the two electrons from the bonding orbital into an antibonding orbital (shown in Fig. 3.17(b)). The wavefunction of this excited state is

$$\Psi_1 = \phi_1(\alpha_a \beta_b + \beta_a \alpha_b) \tag{3.8}$$

which has a symmetric spin part (we ignore the other two triplet spin functions, $\alpha_a\alpha_b$ and $\beta_a\beta_b$, to keep things simple) and an antisymmetric spatial part ϕ_1 , which differs from ϕ_0 because of the antibonding contribution. Mixing of the singlet and triplet states by the contact interaction causes the molecular wavefunction to be a linear combination of Ψ_0 and Ψ_1 (again ignoring normalization constants):

$$\Psi = \Psi_0 + \lambda \Psi_1 = (\phi_0 + \lambda \phi_1) \alpha_a \beta_b - (\phi_0 - \lambda \phi_1) \beta_a \alpha_b$$
(3.9)

where λ is a small constant determined by the strength of the contact interaction and the energy of the excited state Ψ_1 above the ground state Ψ_0 . Since ϕ_0 and ϕ_1 have different shapes (Fig. 3.17), the probability of finding electron a with spin α_a at a given position in the molecule $\left(\sim |\phi_0 + \lambda \phi_1|^2 \right)$ differs from the corresponding probability for $\beta a \left(\sim |\phi_0 - \lambda \phi_1|^2 \right)$. The electronic wavefunction has become *spin-polarized* (Fig. 3.18).

It is now straightforward to see how this leads to an interaction between the two protons (Fig. 3.19). If proton A has spin β , the spin polarization leads to a slight excess of α electron spins and a slight depletion of β electron spins in its vicinity

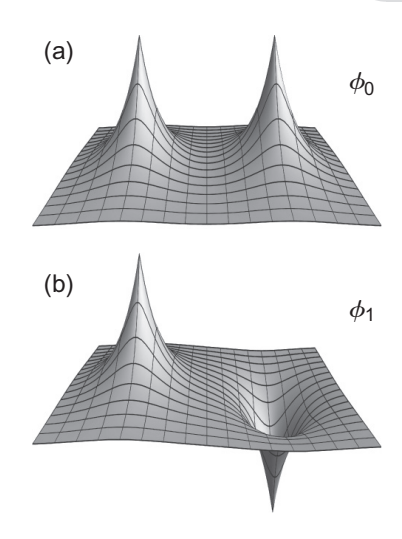


Fig. 3.17 Representations of the bonding (ϕ_0) and antibonding (ϕ_1) molecular orbitals of H_2 (see eqns 3.7 and 3.8).

This description of the origin of spin-spin coupling is a simplified version of one to be found in Carrington and McLachlan (1967).

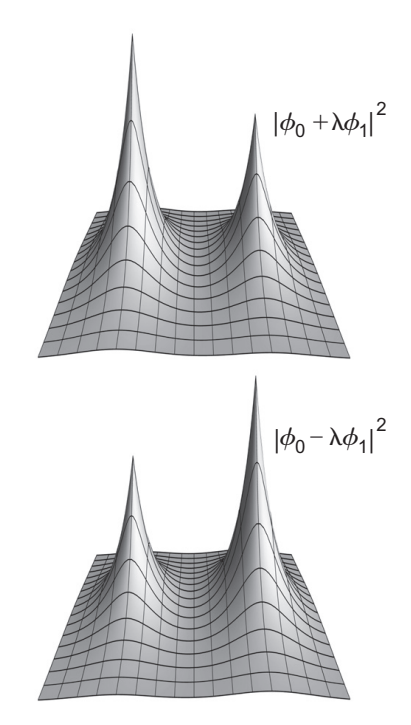
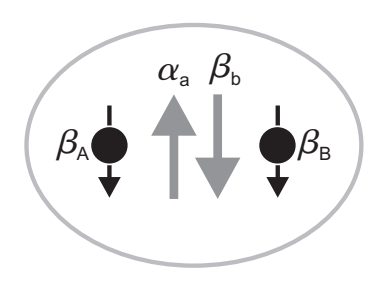


Fig. 3.18 Spin-polarized molecular orbitals of H_2 resulting from Fermi contact interactions. The sketches show the probability of finding an electron in its α spin state ($|\phi_0 + \lambda \phi_1|^2$) and its β spin state ($|\phi_0 - \lambda \phi_1|^2$). The degree of spin polarization has been greatly exaggerated.



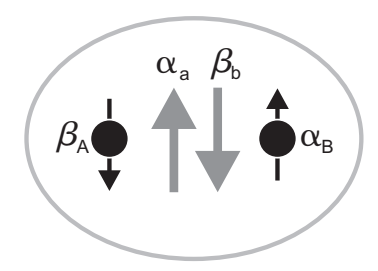


Fig. 3.19 ¹H-¹H *J*-coupling in H₂. Nuclear spins, A and B, are shown as black circles and arrows. Electron spins, a and b, are shown as grey arrows. The lower part of the figure shows the low energy configuration in which the nuclear spins are antiparallel. The upper part shows the high energy configuration with parallel nuclear spins.

(remember that the contact interaction stabilizes antiparallel electron and proton spins). There is a corresponding build-up of β electron spins and reduction of α electron spins near the other proton, B. If B has spin α , it will be stabilized by the local excess of β electron spins through its contact interaction (Fig. 3.18). Conversely, if proton B has spin β , it will be destabilized. In this way one nucleus senses the spin of the other via the valence electrons. If the spin of proton A is inverted, the situation is reversed, and there is a small accumulation of α electron spins around proton B, which is consequently stabilized when it has spin β .

Similar arguments can be used to rationalize the existence of spin-spin interactions in larger molecules. Generally speaking, the strength of the coupling falls off rapidly as the number of intervening bonds increases. In reality, the mechanism of *J*-coupling is rather more complex than suggested by the simple-minded model presented above. Just as with chemical shifts (Section 2.4), it is now possible to calculate *J*-couplings, fairly reliably in many cases, using the methods of *ab initio* quantum chemistry (e.g. Bonhomme *et al.* (2012)). However, in the following paragraphs we discuss a few examples of cases in which *J*-couplings can be related simply and qualitatively to molecular and electronic structure.

3.7 Properties of J-coupling

The highly simplified arguments of the previous section give an impression of the mechanism of spin-spin coupling and indicate its general properties. The strength of the interaction is crucially dependent on the s-character of the wavefunctions of the ground state and electronically excited states at the positions of the nuclei. The coupling is not affected by the strength of the external magnetic field, in contrast to the differences in resonance frequencies that arise from chemical shifts. *J*-couplings are therefore independent of the spectrometer frequency and, being isotropic, are not affected by molecular tumbling.

One-bond and two-bond couplings

The interpretation of the magnitudes of *J*-coupling constants is, in most cases, even more of a problem than it is for chemical shifts, and not one that will be tackled here. Instead, a few representative coupling constants are summarized (Figs 3.20, 3.21, 3.23, and 3.26) together with the briefest of comments.

One-bond carbon-proton couplings (${}^{1}J_{CH}$) generally fall in the range 100–250 Hz, and are sensitive to the s-electron character of the carbon atomic orbital involved in the CH bond, reflecting the crucial role played by the contact interaction. The hydrocarbons ethane, ethylene, and acetylene, which have respectively sp 3 , sp 2 , and sp hybridization, obey the empirical relation:

$$^{1}J_{CH}/Hz \approx 5 \times \%(s) \tag{3.10}$$

where %(s), the percentage s-character of the CH bond, equals 25, 33, and 50 respectively (Fig. 3.20). Similar effects of hybridization are found for strained rings (Fig. 3.20): the smaller the ring size the larger the p-character of the C-C bonds in the ring, and

H_3C-CH_3	125	CH ₄	125	CH ₃ CI	147
$H_2C = CH_2$	157	CH ₃ OH	141	CH ₂ Cl ₂	177
HC≡CH	250	CH ₃ CN	136	CHCl ₃	208
			\triangle		H
123	128	136	161	205	

Fig. 3.20 One-bond ¹³C-¹H coupling constants (in Hz).

Χ $H_2C = CHX$ CH_3-X Н -12.4+2.3Ph +1.3-14.5CI - 1.3 -10.8CN +0.9-16.9

Fig. 3.21 Two-bond ¹H-¹H coupling constants (in Hz).

consequently the larger the s-character of the carbon orbitals used to form the CH bonds. Fig. 3.20 also gives a few examples illustrating the effect of substituents.

Two-bond (geminal) proton-proton couplings vary over a wide range (approximately, -20 to + 40 Hz) with large substituent effects; sp² hybridized CH₂ groups generally have smaller ${}^{2}J_{HH}$ than do methyl groups (Fig. 3.21).

Three-bond couplings

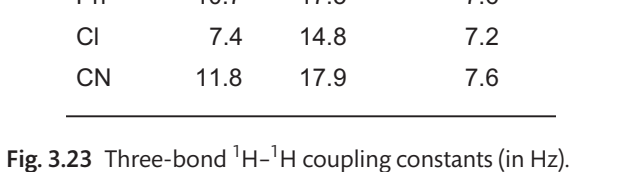
Probably the most useful J-couplings are those involving nuclei separated by three bonds, for example ³J_{HH} in an H-C-C-H fragment. Experimentally and theoretically, these coupling constants are found to vary with the dihedral angle between the two H-C-C planes (θ , see Fig. 3.22) according to the 'Karplus relation':

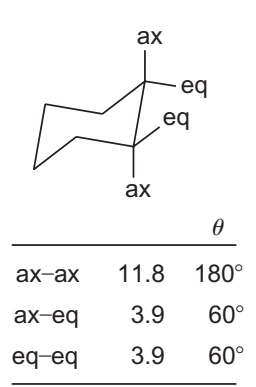
$$^{3}J \approx A + B\cos\theta + C\cos^{2}\theta \tag{3.11}$$

Although it is possible to calculate approximate values for A, B, and C (including substituent and other effects), it is more satisfactory to treat them as coefficients to be determined empirically using conformationally rigid model compounds of known structure. Typical values are A = 2 Hz, B = -1 Hz, C = 10 Hz, which give a θ -variation of the type shown in Fig. 3.22 (a 'Karplus curve'). The values of the three parameters depend on the substituents on the carbon atoms.

The utility of three-bond couplings lies principally in conformational analysis: ³J_{HH} values for the ring protons in cyclohexanes depend on whether axial or equatorial protons are involved; and the trans ¹H-¹H couplings across a C=C bond are up to a factor of two larger than the cis couplings (Fig. 3.23).

	H	= c / H	
	Н	×	CH ₃ CH ₂ —X
Х	cis	trans	
Н	11.5	19.0	8.0
Ph	10.7	17.5	7.6
CI	7.4	14.8	7.2
CN	11.8	17.9	7.6





14 12 10 8 6 4 2 90 180 0 θ / degrees

Fig. 3.22 Typical dependence of a three-bond H-C-C-H coupling constant on the dihedral angle θ .

Fig. 3.24 Part of the backbone of a polypeptide chain, showing the $H-N-C_{\alpha}-H$ dihedral angle. R is the side-chain of the amino acid residue shown in brackets in the lower part of the figure.

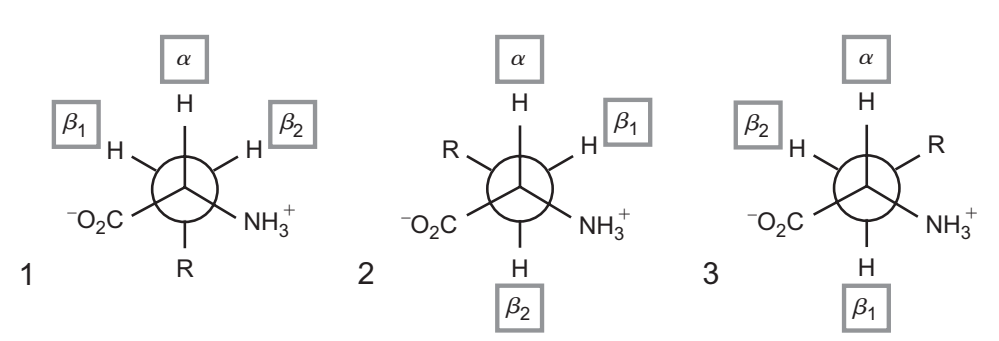


Fig. 3.25 The three staggered conformations of an amino acid shown in Newman projection with C_{α} in front and C_{β} behind.

The Karplus relation finds valuable applications in studies of protein structures. For example, the couplings between the amide (NH) and C_{α} protons in a polypeptide chain provide information on the conformation of the protein backbone (Fig. 3.24). In particular, the two major elements of secondary structure in proteins— α -helices and β -sheets—have characteristic H–N–C $_{\alpha}$ -H dihedral angles: ~120 and ~180° respectively. Thus, $^3J_{\text{HH}}$ values smaller than 6 Hz often indicate an α -helix, while couplings larger than about 7 Hz generally arise from β -sheet regions of the protein.

The interpretation of three-bond couplings in conformationally mobile molecules is somewhat different. Consider, for example, the coupling between the α -proton and the two β -protons in an amino acid (Fig. 3.25). The three staggered conformations, or rotamers, interconvert rapidly so that the two observed ${}^3J_{\alpha\beta}$ values are averages, weighted according to the populations of the three energy minima:

$$J_{\alpha\beta_{1}} = P_{1}J_{g} + P_{2}J_{g} + P_{3}J_{t}$$

$$J_{\alpha\beta_{2}} = P_{1}J_{g} + P_{2}J_{t} + P_{3}J_{g}$$
(3.12)

where $P_1 + P_2 + P_3 = 1$. J_t and J_g are trans ($\theta = 180^\circ$) and gauche ($\theta = \pm 60^\circ$) three-bond coupling constants. Substituent effects on J_t and J_g are ignored here for simplicity. The relative populations of the three rotamers can therefore be determined provided J_t and J_g are available from measurements on rigid model compounds or calculations.

Long-range couplings

Proton-proton coupling constants are generally very small (< 1 Hz) when the nuclei are separated by more than three bonds. A few of the exceptions are shown in Fig. 3.26. Note that large ${}^4J_{HH}$ and ${}^5J_{HH}$ often occur when the coupling is transmitted along a zigzag arrangement of bonds and/or through π -bonds.

$$^{5}J_{HH} = +2.2$$
 $H-C \equiv C-C \equiv C-H$
 $^{7}J_{HH} = -1.3$
 $^{7}J_{HH} = -1.3$

Fig. 3.26 Long range ¹H-¹H coupling constants (in Hz).

3.8 Dipolar coupling

Finally, we turn to the direct dipolar interactions between nuclei which, though not normally responsible for splittings in the spectra of molecules in the liquid state, are important in solid-state NMR and for spin relaxation (Chapter 5). The basic features of dipolar interactions are presented in Appendix A.

Dipolar interaction in solids

Eqn A.2 in Appendix A gives an expression for the energy of interaction of two classical magnetic moments, μ_A and μ_X , both pointing along the positivez-axis:

$$E = -\left(\frac{\mu_0}{4\pi}\right) \left(\frac{\mu_A \mu_X}{r^3}\right) \left(3\cos^2\theta - 1\right) \tag{3.13}$$

where r is the internuclear distance, θ is the angle between the internuclear vector and the z-axis, and $\mu_0 = 4\pi \times 10^{-7}$ H m⁻¹ is the vacuum permeability.

We consider first the heteronuclearcase in which A and X are spin- $\frac{1}{2}$ nuclei with different magnetogyric ratios ($\gamma_A \neq \gamma_X$). In the strong magnetic field of an NMR spectrometer, both spins are quantized along the field direction (the z-axis). To make eqn 3.13 applicable to nuclear spins (i.e. quantum rather than classical magnetic moments), we can just replace μ_A and μ_X by their z-components, $\gamma_A m_A \hbar$ and $\gamma_X m_X \hbar$ respectively (using $\mu_Z = \gamma_{L_Z}$ and $L_Z = m\hbar$ as in Chapter 1). This gives

$$E = -hR_{AX}(3\cos^2\theta - 1)m_Am_X \tag{3.14}$$

where

$$R_{AX} = \left(\frac{\hbar}{2\pi}\right) \left(\frac{\mu_0}{4\pi}\right) \left(\frac{\gamma_A \gamma_X}{r^3}\right) \tag{3.15}$$

is the dipolar coupling constant (in Hz). Comparing eqn 3.14 with the corresponding expression for a pair of weakly J-coupled spins (eqn 3.1), one can see that the NMR signals of A and X will both be doublets with a splitting

$$R_{AX}(3\cos^2\theta - 1). \tag{3.16}$$

For example, if the two nuclei are 1 H and 13 C, RCH = 8,951 Hz when r = 1.5 Å; 472 Hz at 4 Å; and 30 Hz at 10 Å. Compared to 1 J-couplings, dipolar interactions are strong and long range.

Figure 3.27 shows NMR spectra calculated for a range of values of θ between 0° and 90°. These are the sort of spectra that would be observed for isolated AX pairs in a single crystal as the crystal is rotated in the magnetic field of the spectrometer. As θ changes from 0° ($3\cos^2\theta - 1 = 2$) to 90° ($3\cos^2\theta - 1 = -1$) the doublet splitting decreases, goes through zero at 54.7° (the so-called magic angle) and then increases again as θ rises to 90°. Identical behaviour is found in both the A and X spectra. Internuclear separations may easily be determined from single crystal spectra of such simple spin systems.

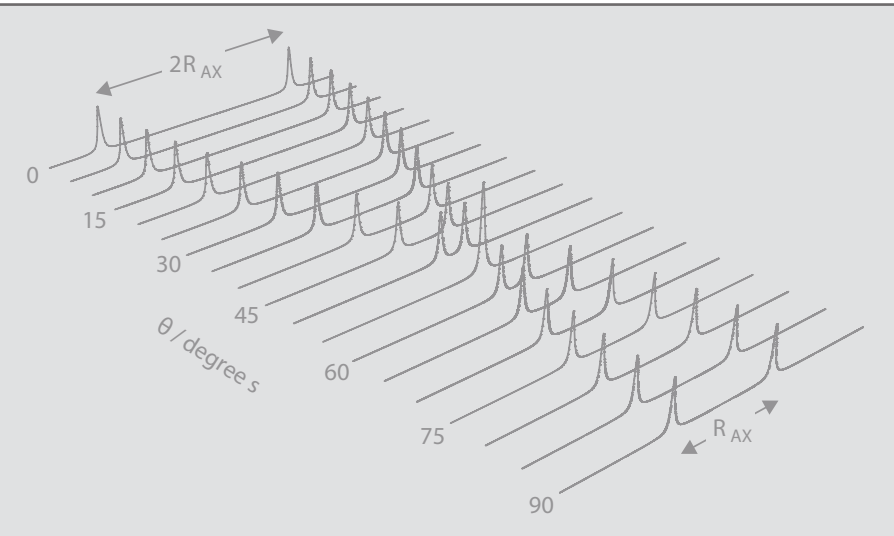


Fig. 3.27 Calculated NMR spectra for one member of a heteronuclear pair (AX) of dipolar-coupled spin- $\frac{1}{2}$ nuclei. θ is the angle between the internuclear vector and the magnetic field direction. The dipolar coupling constant R_{AX} is given by eqn 3.15.

The situation is a bit more complicated for a powdered sample. Although each AX pair has a unique value of θ , different molecules have different θ . Assuming a random distribution of orientations, the observed 'powder spectrum 'is the sum of the single crystal spectra for θ between 0 and 90°, each weighted by $\sin\theta$ to take into account the probability of finding an AX pair with orientation θ . Adding these spectra together produces the unusual lineshape shown in Fig. 3.28: the 'horns' correspond to $\theta \approx 90^\circ$, while the wings come from the $\theta \approx 0^\circ$ orientations.

As may be anticipated, both single crystal and powder spectra are somewhat more complicated for larger spin systems, where each nucleus may have significant dipolar interactions with many neighbouring spins, each with its ownr and θ .

Homonuclear dipolar couplings, between spins with the same γ , produce single crystal and powder spectra that are essentially identical to those arising from heteronuclear interactions. The only difference is that the doublet splitting contains an extra factor of $\frac{3}{2}$:

$$\frac{3}{2}R_{AX}\left(3\cos^2\theta - 1\right) \text{ and } R_{AX} = \left(\frac{\hbar}{2\pi}\right)\left(\frac{\mu_0}{4\pi}\right)\left(\frac{\gamma^2}{r^3}\right). \tag{3.17}$$

Briefly, the $\frac{3}{2}$ arises because the homonuclear dipolar interaction mixes the spin states $\alpha_A\beta_X$ and $\beta_A\alpha_X$. This does not occur in the heteronuclear case because the energy gap between $\alpha_A\beta_X$ and $\beta_A\alpha_X$ ($\approx\hbar|\gamma_A-\gamma_X|B_0$) is much greater than the strength of the coupling (\approx hR_{AX}). The effect is very similar to the mixing that occurs for strongly J-coupled spins (Section 3.5); however the form of the dipolar coupling changes the details of the mixing such that dipolar splittingsare observed for equivalent nuclei. For example, the ¹H NMR spectrum of an isolated water molecule in a crystal is a doublet with splitting given by eqn 3.17 (R_{HH} = 30.5 kHz for r = 1.58 Å).

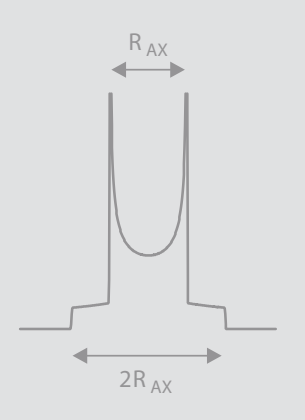


Fig. 3.28 Calculated powder spectrum for one member of a heteronuclear pair of dipolar-coupled spin- $\frac{1}{2}$ nuclei. This lineshape is often referred to as a 'Pake pattern'.

SPIN – SPIN COUPLING 45

Dipolar interaction in liquids

Evidently dipolar couplings have a profound effect on the NMR spectra of solids, but what about liquids with which this book is principally concerned?

Molecules in liquids rotate rapidly with frequent changes in the axis and speed of rotation as a result of collisions with other molecules. Consequently, for any pair of nuclei, the angle θ and therefore their dipolar interaction are rapidly modulated. As discussed in more detail in Section 5.6, this leads to an average splitting, provided the average rotational frequency greatly exceeds the strength of the dipolar coupling. This condition is certainly met for all but very large molecules and/or very viscous solutions. For example, a water molecule at room temperature has a rotation frequency of $\sim 10^{12}$ Hz, while the largest dipolar couplings are no more than 10^5 Hz. To obtain the dipolar splitting of a molecule in a liquid, the angular parts of eqns 3.16 and 3.17 must therefore be averaged over all molecular orientations, θ :

splitting =
$$\lambda R_{AX} \int_0^{\pi/2} (3\cos^2 \theta - 1) \sin \theta \, d\theta$$
 (3.18)

where $\sin\theta$ is the appropriate weighting factor for a molecule that has no preferred orientation and λ equals 1 for heteronuclear spins (eqn 3.16) and $\frac{3}{2}$ for homonuclear spins (eqn 3.17). This integral is identically zero: the positive parts of the integrand ($0 \le \theta \le 54.7^\circ$) exactly cancel the negative parts ($54.7^\circ \le \theta \le 90^\circ$). Thus, dipolar interactions do not normally produce splittings in the NMR spectra of liquids. (But they do play a crucial role in spin relaxation as we shall see in Chapter 5.)

However, the $\sin\theta$ weighting factor in eqn 3.18 is not always appropriate. When molecules are partially aligned with respect to the magnetic field B_0 , the average dipolar splitting does not vanish because the positive and negative parts of the integrand no longer exactly cancel. This can come about when the interaction of the molecules with B_0 is anisotropic such that certain molecular orientations have lower energy and are thus more prevalent than others. Alternatively, molecules can be partially aligned if they are dissolved in a medium that is itself aligned with B_0 . Examples of such media include solutions of rod-shaped viruses or disc-shaped assemblies of phospholipids (known as bicelles) and stretched or compressed polyacrylamide gels (Cavanaghet al. (2007)). Under such conditions, the measured spin–spin coupling of two nuclear spins will be

splitting =
$$J_{AX} - \lambda R_{AX} \langle 3\cos^2 \theta - 1 \rangle$$
 (3.19)

where J_{AX} is the J-coupling, and the angled brackets indicate the orientational average. These residual dipolar coupling provide valuable information on the orientation of internuclear vectors within molecules. The idea is to tune the degree of molecular alignment such that only the spin–spin couplings (eqn 3.19) of directly bonded atoms are affected. Knowing the bond-lengths, it is then possible to determine the relative orientations of, for example, all the backbone amide $^1H^{-15}N$ bonds within a protein. When allied with nuclear Overhauser enhancements (Section 5.8) and torsion angles from three-bond J-couplings (Section 3.7), residual dipolar couplings provide a powerful method for protein structure determination (see e.g. Kwanet al. (2011)).

The properties of J- and dipolar couplings are summarized in Table 3.4.

Molecules tend to orient in a magnetic field when their magnetic susceptibilities are significantly anisotropic, i.e. when the field induces a magnetic moment in the molecule that depends on its orientation. Molecules containing paramagnetic metal atoms often have large anisotropic magnetic susceptibilities.

J-couplings	Dipolar couplings
Through bonds	Through space
Strength < 100 Hz	Strength < 100 kHz
Isotropic	3cos² <i>θ</i> − 1
Small for > 3 bonds ^a	1/r ³
Cause splitting in spectra	Splitting for solids and partially aligned molecules in liquid
Do not cause relaxation	Cause relaxation when motion present

Unless modulated by internal motion.

3.9 Summary

Spin–spin interactions (J-couplings) give rise to multiplets in liquid-state NMR spectra.

Jecoupling usually occurs via chemical bonds and is generally small when the nuclei are more than three bonds apart.

J-couplings give information on bonding networks in molecules.

Jecouplings within a group of magnetically equivalent spins do not produce multiplet splittings.

Strongly coupled spins have more complex spectra than weakly coupled spins.

Dipolar couplings occur through space and normally do not lead to multiplets in liquid-state NMR spectra.

3.10 Exercises

Answers to the exercises are provided at the back of the book. Full worked solutions are available on the Online Resource Centre at < URL >

- 1. Suggest structures for the following compounds based on the multiplets observed in their NMR spectra (ignore spin–spin couplings involving Cl and I): (a) ^{19}F spectrum of CIF₃: doublet and triplet. (b) ^{19}F spectrum of IF₅: doublet and quintet. (c) ^{1}H spectrum of C $_{3}H_{7}Cl$: doublet and septet. (d) ^{1}H spectrum of C $_{2}H_{3}OCl$: three doublets of doublets. (e) The ^{51}V spectrum of VOF_{4}^{-} is a quintet. The ^{19}F spectrum comprises eight equally spaced lines with the same intensity. Propose a structure for VOF_{4}^{-} and determine the spin quantum number of ^{51}V .
- Predict the total number of lines in the ¹H spectra of the following compounds: (a) CH₃Cl. (b) (CH₃)₃CH. (c) 1,4-dichloro-2,3-dibromobenzene. (d) 1,2-dichloro-3,4-dibromobenzene. (e) 1,1-dichlorocyclopropane. Assume that all J-couplings involving Br and Cl are negligibly small.

- 3. The ¹H spectrum of CH ₂D₂ contains five lines. What are their relative intensities? (b) How many lines are there in the ¹H spectrum of CHD ₃?
- 4. The ¹H spectra of which isomers of C₄H₉Cl contain the following multiplets? (a) doublet, triplet, quintet, and sextet; (b) triplet, triplet, quintet, and sextet. Assume all three-bond J_{HH} are identical and ignore all other couplings.
- 5. What would the spectrum in Fig. 3.13 look like if all the lines had widths of 3 Hz?
- 6. The ¹H spectrum of an AX spin system has lines at the following frequencies: -600.001677, -600.001683, -600.004437, -600.004443 MHz. Taking the Larmor frequency of TMS to be exactly -600 MHz, determine the two chemical shifts and the J-coupling.
- 7. For each of the following compounds determine whether the protons are magnetically or chemically equivalent. (a) benzene. (b) the 2,5 protons in furan. (c) $F_2C=C=CH_2$. (d) $H^{-13}C^{-13}C-H$.
- 8. The protons in 2-bromo-5-chlorothiophene have a chemical shift difference of 0.154 ppm and a J-coupling of 3.9 Hz. Determine the ratio of the intensities of the inner and outer lines of the four-line ¹H spectrum on (a) a 600 MHz and (b) a 40 MHz spectrometer.
- 9. The ${}^{1}\text{H}-{}^{1}\text{H}$ J-coupling in a compound CHX ${}_{2}$ -CHY ${}_{2}$ is 3.46 Hz. If J = 2.2Hz and J ${}_{1}$ = 9.7Hz, determine the mole fractions of the two rotamers.
- 10. 13 C NMR spectra of a single crystal of isotopically enriched glycine, 15 NH $_3^{+-13}$ CH $_2^{--13}$ CO $_2^{-}$, were measured for different orientations of the crystal. The maximum 15 N 13 CH $_2$ and 13 C– 13 C dipolar splittings were found to be 1.941 kHz and 6.414 kHz respectively. Determine (a) the C–C and (b) the C–N bond lengths.